

# Self-Organized Formation of GaSb/GaAs Quantum Rings

R. Timm,<sup>1,\*</sup> H. Eisele,<sup>1,2</sup> A. Lenz,<sup>1</sup> L. Ivanova,<sup>1</sup> G. Balakrishnan,<sup>3</sup> D.L. Huffaker,<sup>3,†</sup> and M. Dähne<sup>1</sup>

<sup>1</sup>*Institut für Festkörperphysik, Technische Universität Berlin, 10623 Berlin, Germany*

<sup>2</sup>*Department of Physics, University of Texas at Austin, Austin, Texas 78712, USA*

<sup>3</sup>*Center for High Technology Materials, University of New Mexico, Albuquerque, New Mexico 87106, USA*

(Received 22 July 2008; published 16 December 2008)

Ring-shaped GaSb/GaAs quantum dots, grown by molecular beam epitaxy, were studied using cross-sectional scanning tunneling microscopy. These quantum rings have an outer shape of a truncated pyramid with baselengths around 15 nm and heights of about 2 nm but are characterized by a clear central opening extending over about 40% of the outer baselength. They form spontaneously during the growth and subsequent continuous capping of GaSb/GaAs quantum dots due to the large strain and substantial As-for-Sb exchange reactions leading to strong Sb segregation.

DOI: 10.1103/PhysRevLett.101.256101

PACS numbers: 81.07.Ta, 68.37.Ef, 68.65.Hb, 81.16.Dn

The transition of self-assembled semiconductor quantum dots (QDs) with a compact, conventional shape into toroidal QD structures—so-called quantum rings (QRs)—has attracted increasing interest during the past years [1], especially because such QRs exhibit unique properties, e.g., quantum-mechanical Aharonov-Bohm oscillations [2]. In the In(Ga)As/GaAs and most other material systems, the ringlike structure is obtained after partially capping the initially compact QDs by a thin overlayer, followed by a growth interruption (GI) for annealing. However, the resulting structures typically are not actual rings but are characterized by a craterlike shape with a solid bottom and a slightly higher rim [3,4].

Here we present cross-sectional scanning tunneling microscopy (XSTM) results on GaSb QRs in GaAs, showing a toroidal shape with a clear central opening filled with GaAs. These QRs form during the growth and subsequent fast overgrowth of GaSb QDs without additional GI steps and for various amounts of deposited QD material. GaSb/GaAs nanostructures are characterized by a staggered type-II band alignment with a large hole confinement [5], making this QD system very promising both for applications like charge storage devices [6] as well as for a strong Aharonov-Bohm effect especially in QRs [7].

Up to now, mainly uncovered GaSb/GaAs QDs have been structurally investigated in top-view geometry, typically showing a compact shape without a central opening or depression [8,9]. While small QDs grown by metal-organic chemical vapor deposition preserve this compact shape upon capping [10], for large uncovered GaSb QDs grown by molecular beam epitaxy (MBE), first indications for a ringlike shape have been reported [11]. Here we clearly demonstrate the ring structure of capped GaSb QDs with atomic resolution and can furthermore relate this shape transition to the high strain energy and strong segregation effects upon overgrowth.

The investigated sample, grown by MBE using As<sub>2</sub> and Sb<sub>4</sub> at a growth rate of 0.3 ML/s, consists of four GaSb layers, 1.0, 2.0, 2.7, and 3.1 ML thick, separated by

~100 nm thick GaAs spacer layers. Each GaSb layer was preceded by a 15 s long GI with the last 5 s under Sb pressure, representing the so-called Sb-soaking step during which expectedly about one monolayer (ML) As was replaced by Sb at the growth surface [9,12]. The growth temperature was 490 °C for the GaSb layers and the following 5–10 nm of GaAs and 550 °C for the remaining GaAs. Reflection high energy electron diffraction showed a clear QD signal for all four GaSb layers during growth.

For the XSTM measurements, different specimens of the sample were cleaved in ultrahigh vacuum, resulting in (110) or ( $\bar{1}10$ ) surfaces, and analyzed using a homebuilt STM with an RHK Technology SPM 1000 control electronics. Electrochemically etched tungsten tips were employed, cleaned *in situ* by electron bombardment. Sample voltages between  $-1.8$  and  $-2.6$  V and tunneling currents of 50–90 pA were used.

A typical XSTM overview image of a GaSb QD layer is shown in Fig. 1(a). Because of the negative sample voltage, the filled states belonging to the group-V atoms of the atomic zigzag chains along  $[\bar{1}10]$  direction are imaged. Even single Sb atoms can be detected, which appear

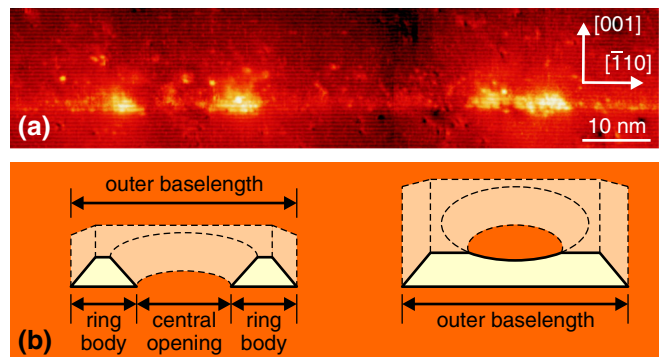


FIG. 1 (color online). (a) Overview filled-state XSTM image of GaSb QD layer 3, showing two QRs cleaved at different positions, as sketched in (b).

brighter than As atoms due to the electronic image contrast [13,14]. Within the strongly intermixed and partly interrupted wetting layer (WL), two QD structures of different appearance dominate the image contrast due to their strain relaxation, leading to a structural protrusion out of the cleavage surface [10,15]. The paired feature at the left is a clear cross section through a QR, as sketched in Fig. 1(b). The rather trapezoidal feature at the right suggests a cross section through a compact QD with a truncated pyramidal shape but can even better be related to a ring structure which is cleaved off center [Fig. 1(b)], as demonstrated in the following.

Figure 2 shows close views of such GaSb nanostructures. The QRs in Figs. 2(a) and 2(b) exhibit a well-defined ring body consisting of rather pure GaSb and a large central opening filled with almost Sb-free GaAs. Even the QD in Fig. 2(c) with its almost trapezoidal cross section already shows indications for a ring shape: If a QR is cleaved close to the edge, as sketched in Fig. 1(b), a weaker strain-induced XSTM image contrast right in the center than at its sides is expected, and a larger vertical extension near the sides than at the center of the cross section can result, in excellent agreement with Fig. 2(c).

In order to investigate the QR structure more quantitatively and to determine whether all QDs are ring-shaped, XSTM images of 140 QDs in all four GaSb layers were analyzed. 69 QDs appeared compact and 71 as paired features. Also, the ratio  $r_{app}$  between the apparent lateral extension  $d_{app}$  of the central opening and the outer baselength  $b$  (see inset in Fig. 3) was determined from the

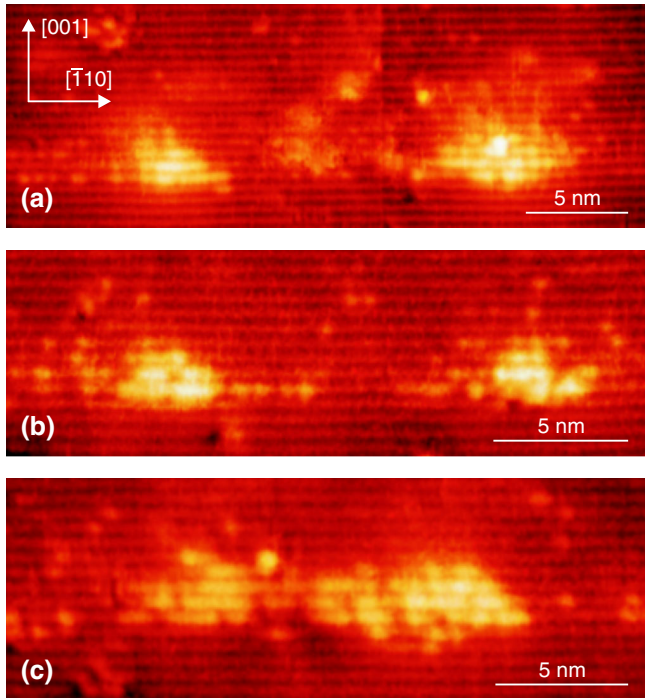


FIG. 2 (color online). Close-view filled-state XSTM images of GaSb QRs in layer 3, (a),(b) cleaved centrally and (c) close to the edge.

XSTM images. This ratio is independent of the varying total QD size. The experimental distribution of  $r_{app}$ , which is almost the same for all four GaSb layers, is displayed by the orange bars in Fig. 3. It was then simulated assuming that all QDs are ring-shaped with a square base and a circular opening [16]. For this calculation, a Gaussian distribution of the actual ratio  $r_{actual}$  between the inner QR diameter and its baselength was assumed with an average value  $r_0$  and a standard deviation  $\sigma$ , and randomly distributed cleavage positions were considered, resulting in the distribution shown by the blue bars. The very good agreement with the experimental histogram and the fact that the experimental peak for  $r_{app} = 0$ , representing the QDs with a compact appearance in the XSTM images, does not exceed the calculated value clearly demonstrate that all QDs are actually ring-shaped. The even smaller experimental peak at  $r_{app} = 0$  indicates that in those cases where the largest part of the QR is cleaved away the remainder has not always been detected in the XSTM images due to its strongly decreased strain relaxation and a therewith weak image contrast. From the best fit of the simulated Gaussian distribution, the average inner diameter of the QRs is obtained to 42% of the outer baselength and the standard deviation to 13%.

The outer shape of the QRs is that of a truncated pyramid, as can be seen in Fig. 2. Comparing the XSTM results of the (110) and  $(\bar{1}\bar{1}0)$  cleavage surface, no asymmetry of the QRs is found. From the fact that the centrally cleaved QRs (appearing as a paired feature in the XSTM images) and those cleaved near its edge (with a compact appearance) have about the same average lateral extension, a square base can be concluded for the truncated pyramid. In addition, the measured values of the inclination angle between the QR base and the outer side facets in the XSTM

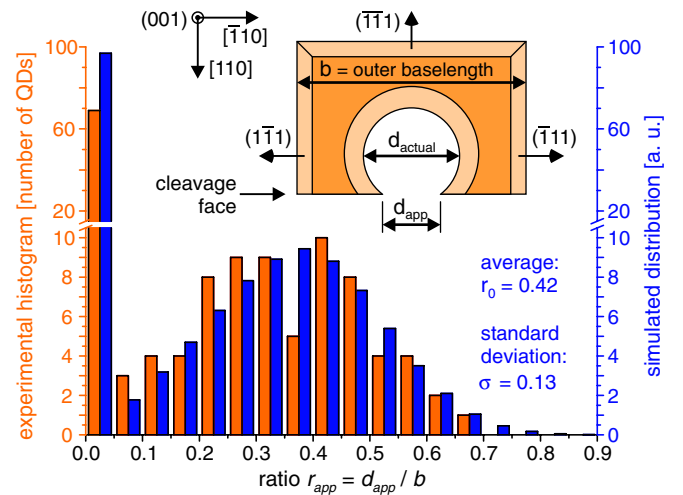


FIG. 3 (color online). Distribution of the ratio  $r_{app}$  of apparent inner ring diameter  $d_{app}$  to outer baselength  $b$ , obtained from the XSTM images (orange columns, left) and from a simulation (blue columns, right) using the indicated parameters  $r_0$  and  $\sigma$ . The shape of a cleaved QR is shown in the inset.

TABLE I. QR sizes and densities in layers 1–4.

Layer	Deposited GaSb [ML]	Baselength [nm]	Height [nm]	Density [ $10^{10} \text{ cm}^{-2}$ ]
1	1.0	$12.7 \pm 4.1$	$1.6 \pm 0.3$	$4.3 \pm 0.8$
2	2.0	$16.3 \pm 4.9$	$2.0 \pm 0.3$	$7.3 \pm 1.0$
3	2.7	$15.4 \pm 4.3$	$2.1 \pm 0.4$	$8.1 \pm 1.3$
4	3.1	$15.2 \pm 4.0$	$2.1 \pm 0.3$	$9.3 \pm 2.0$

images of about  $50^\circ$  indicate  $\{111\}$  side facets with a nominal angle of  $54.7^\circ$ . The resulting shape is sketched in the inset in Fig. 3.

Table I shows the QR sizes and densities, derived from all 140 QRs. With an increasing amount of deposited GaSb in layers 1–4, the density increases by a factor of 2, nearly reaching  $10^{11} \text{ cm}^{-2}$ . The average QR size, however, increases only from layers 1–2 and remains constant thereafter with baselengths of in average 16 nm and heights of about 2 nm.

Also, the chemical composition of the QRs was analyzed by evaluating the distance between neighboring atomic chains in growth direction. By comparing this local lattice constant with simulations of the strain relaxation based on continuum mechanics on an atomic scale, the local stoichiometry is obtained [10,15]. This is shown for a typical QR in Fig. 4(a): Within the QR body, the GaSb composition varies between about 70% and pure material, while in the WL a maximum GaSb composition of only about 20% is reached [17]. A significant undershoot of the chain distances underneath the QR body demonstrates the large strain, compressing also the surrounding GaAs. From the absence of such an undershoot above the QR—in one region, the chain distance even remains increased over several atomic chains—a sharp interface between the GaSb QR and the GaAs overlayer can be excluded, indicating strong Sb segregation.

Indeed, many individual Sb atoms can be observed as bright spots above the WL and the QRs in Fig. 2. By counting such segregated atoms, the GaSb content of the atomic chains above the WL was evaluated, resulting in a clear exponential decay, as shown in Fig. 4(b). It was demonstrated that an Sb floating layer is formed at the growth front upon overgrowth [17]. One part of these floating Sb atoms gets reincorporated with a constant fraction of 16% per GaAs ML, leading to the observed exponential segregation profile [17,18]. It was found, however, that the total amount of GaSb in every QR layer after capping, including these segregated atoms, is limited to about 2 ML due to strain [17]. Thus, the remaining part of the Sb floating layer stays at the growth front without being incorporated, acting as a surfactant [14,17].

The Sb atoms of the floating layer are provided by strong As-for-Sb exchange reactions at the GaSb growth surface when starting the GaAs overgrowth, i.e., when the group-V species is switched from Sb to As. Very Sb-rich surface reconstructions of the GaSb layer and a comparatively

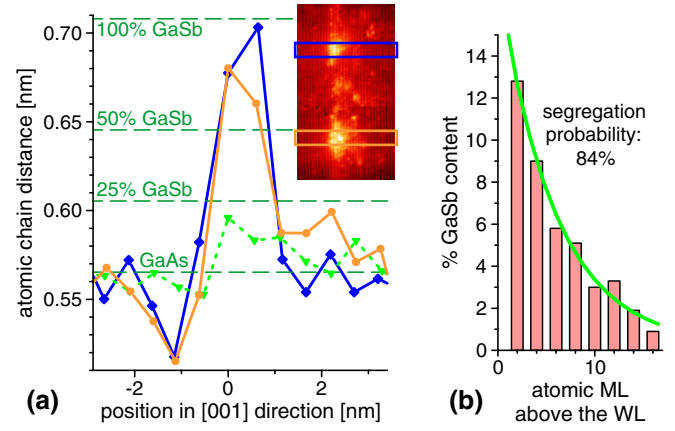


FIG. 4 (color online). Analysis of the chemical composition: (a) Variation of the lattice constant in the growth direction for different regions of the QR shown in the inset (solid blue and orange curves) as well as of the WL (dotted green curve) and calculated values for  $\text{GaSb}_x\text{As}_{1-x}$  quantum wells (dashed green lines). (b) GaSb content of the atomic chains above the WL base evaluated by atom counting, showing an exponential decay fitted by the green curve. Note that the atomic chains in the XSTM images represent only every second ML.

weak Ga–Sb bond [19] contribute to this substantial group-V exchange process [17]. Even more, an Sb-covered GaAs(001) surface has been found to partly relieve strain, leading to a low surface energy [20], which favors the occurrence of an Sb floating layer.

In the following, we discuss why the ring formation during growth and subsequent fast overgrowth of QDs occurs, in particular, for the GaSb/GaAs system, and why this QR structure comes much closer to an ideal ring shape than the craterlike InAs/GaAs structures [3,4]. This can mainly be attributed to the strain energy [21], which is significantly reduced when a compact QD is transformed into a QR, since therewith especially the strain at its center gets decreased. Furthermore, the strain within the QDs increases drastically upon capping as they are forced to fit completely into the GaAs atomic lattice.

At GaSb/GaAs nanostructures, the strain energy is particularly high: For model systems consisting of 1 ML thick GaSb/GaAs or InAs/GaAs WLs, we applied atomistic continuum mechanics [22] to calculate the strain energy, using the material lattice constants and elastic moduli [23]. The resulting strain energy amounts to 1.87 eV for each Ga–Sb atom pair in contrast to 1.40 eV for each In–As pair. Although the lattice mismatch for GaSb/GaAs is only 8% larger than for InAs/GaAs, the total strain energy is 34% larger due to the different elastic moduli. Thus the driving force for complete ring formation is much higher for GaSb/GaAs than for InAs/GaAs. This difference in strain energy is also reflected by the typical sizes of capped QDs, amounting to about 15–20 nm for compact InAs/GaAs QDs [15,24] and slightly above 20 nm for InAs/GaAs ringlike structures [3] but only 12–17 nm for the GaSb/GaAs QRs studied here.



The GaSb/GaAs QR formation is further supported by the strong segregation kinetics manifested by the extensive As-for-Sb exchange process described above, favoring the fast repulsion of Sb atoms from the highly strained QD centers, where they are replaced by As.

For extremely large GaSb/GaAs QDs and appropriate growth conditions, the strain energy can even get so high that QRs are formed prior to any overgrowth step, as it is reported in Ref. [11]. In most cases, however, uncapped GaSb/GaAs QDs have a conventional, compact shape [8,9,25]. For the capped QDs studied here, the same distribution of inner ring diameter to outer baselength was observed for different amounts of deposited GaSb material, even for only 1 ML GaSb growth following 5 s Sb soaking, demonstrating that the ring formation is not limited to large structures if the QDs are capped.

In conclusion, we revealed the formation process and the atomic structure of MBE-grown GaSb/GaAs QRs using XSTM. The QRs have an outer shape of a square-based truncated pyramid with {111} side facets and a clear central opening extending in average over 42% of the baselength. They form spontaneously during QD growth and subsequent fast and continuous capping due to the high strain energy and substantial As-for-Sb exchange reactions leading to strong Sb segregation.

This work was funded by Projects No. Da408/13, SFB 296, and SFB 787 of the Deutsche Forschungsgemeinschaft and by the SANDiE NoE of the European Commission. Two of the authors (H. E. and D. L. H.) acknowledge financial support from the Humboldt Foundation.

---

\*timm@physik.tu-berlin.de

†Present address: California NanoSystems Institute, University of California, Los Angeles, CA 90095, USA.

- [1] D. Granados and J. M. García, Appl. Phys. Lett. **82**, 2401 (2003); T. Raz, D. Ritter, and G. Bahir, Appl. Phys. Lett. **82**, 1706 (2003); M. Sztucki, T. H. Metzger, V. Chamard, A. Hesse, and V. Holý, J. Appl. Phys. **99**, 033519 (2006); H.-S. Ling and C.-P. Lee, J. Appl. Phys. **102**, 024314 (2007).
- [2] Y. Aharonov and D. Bohm, Phys. Rev. **115**, 485 (1959); A. Lorke, R. J. Luyken, A. O. Govorov, J. P. Kotthaus, J. M. García, and P. M. Petroff, Phys. Rev. Lett. **84**, 2223 (2000); N. A. J. M. Kleemans, I. M. A. Bomiñaar-Silkens, V. M. Fomin, V. N. Gladilin, D. Granados, A. G. Taboada, J. M. García, P. Offermans, U. Zeitler, P. C. M. Christianen, J. C. Maan, J. T. Devreese, and P. M. Koenraad, Phys. Rev. Lett. **99**, 146808 (2007).
- [3] P. Offermans, P. M. Koenraad, J. H. Wolter, D. Granados, J. M. García, V. M. Fomin, V. N. Gladilin, and J. T. Devreese, Appl. Phys. Lett. **87**, 131902 (2005).
- [4] G. Costantini, A. Rastelli, C. Manzano, P. Acosta-Díaz, R. Songmuang, G. Katsaros, O. G. Schmidt, and K. Kern, Phys. Rev. Lett. **96**, 226106 (2006); A. Lenz, H. Eisele, R. Timm, S. K. Becker, R. L. Sellin, U. W. Pohl, D. Bimberg, and M. Dähne, Appl. Phys. Lett. **85**, 3848 (2004).
- [5] F. Hatami, N. N. Ledentsov, M. Grundmann, J. Böhrer, F. Heinrichsdorff, M. Beer, D. Bimberg, S. S. Ruvimov, P. Werner, U. Gösele, J. Heydenreich, U. Richter, S. V. Ivanov, B. Ya. Meltser, P. S. Kop'ev, and Zh. I. Alferov, Appl. Phys. Lett. **67**, 656 (1995).
- [6] M. Geller, C. Kapteyn, L. Müller-Kirsch, R. Heitz, and D. Bimberg, Appl. Phys. Lett. **82**, 2706 (2003).
- [7] M. Grochol, F. Grosse, and R. Zimmermann, Phys. Rev. B **74**, 115416 (2006).
- [8] P. M. Thibado, B. R. Bennett, M. E. Twigg, B. V. Shanabrook, and L. J. Whitman, J. Vac. Sci. Technol. A **14**, 885 (1996); G. Balakrishnan, J. Tatebayashi, A. Khoshakhlagh, S. H. Huang, A. Jallipalli, L. R. Dawson, and D. L. Huffaker, Appl. Phys. Lett. **89**, 161104 (2006).
- [9] K. Suzuki, R. A. Hogg, and Y. Arakawa, J. Appl. Phys. **85**, 8349 (1999).
- [10] R. Timm, H. Eisele, A. Lenz, S. K. Becker, J. Grabowski, T.-Y. Kim, L. Müller-Kirsch, K. Pötschke, U. W. Pohl, D. Bimberg, and M. Dähne, Appl. Phys. Lett. **85**, 5890 (2004); R. Timm, J. Grabowski, H. Eisele, A. Lenz, S. K. Becker, L. Müller-Kirsch, K. Pötschke, U. W. Pohl, D. Bimberg, and M. Dähne, Physica E (Amsterdam) **26**, 231 (2005).
- [11] S. Kobayashi, C. Jiang, T. Kawazu, and H. Sakaki, Jpn. J. Appl. Phys. **43**, L662 (2004).
- [12] I. Farrer, M. J. Murphy, D. A. Ritchie, and A. J. Shields, J. Cryst. Growth **251**, 771 (2003).
- [13] R. M. Feenstra, J. A. Stroscio, J. Tersoff, and A. P. Fein, Phys. Rev. Lett. **58**, 1192 (1987).
- [14] R. Timm, H. Eisele, A. Lenz, T.-Y. Kim, F. Streicher, K. Pötschke, U. W. Pohl, D. Bimberg, and M. Dähne, Physica (Amsterdam) **32E**, 25 (2006).
- [15] O. Flebbe, H. Eisele, T. Kalka, F. Heinrichsdorff, A. Krost, D. Bimberg, and M. Dähne-Prietsch, J. Vac. Sci. Technol. B **17**, 1639 (1999).
- [16] The choice of either a square or a circular base has only marginal influence on the calculated distribution.
- [17] R. Timm, A. Lenz, H. Eisele, L. Ivanova, M. Dähne, G. Balakrishnan, D. L. Huffaker, I. Farrer, and D. A. Ritchie, J. Vac. Sci. Technol. B **26**, 1492 (2008).
- [18] J. Steinshnider, J. Harper, M. Weimer, C.-H. Lin, S. S. Pei, and D. H. Chow, Phys. Rev. Lett. **85**, 4562 (2000).
- [19] J. M. Ulloa, I. W. D. Drouzas, P. M. Koenraad, D. J. Mowbray, M. J. Steer, H. Y. Liu, and M. Hopkinson, Appl. Phys. Lett. **90**, 213105 (2007).
- [20] J. E. Bickel, N. A. Modine, C. Pearson, and J. Mirecki Millunchick, Phys. Rev. B **77**, 125308 (2008).
- [21] This fully elastic approach is justified since plastic relaxation can be excluded from the XSTM data.
- [22] J. F. Nye, *Physical Properties of Crystals* (Clarendon Press, Oxford, 1972); H. Eisele, O. Flebbe, T. Kalka, and M. Dähne-Prietsch, Surf. Interface Anal. **27**, 537 (1999).
- [23] *Numerical Data and Functional Relationships in Science and Technology*, Landolt-Börnstein New Series, Group III, Vol. 17a (Springer, Berlin, 1982).
- [24] M. Dähne, H. Eisele, and K. Jacobi, in *Semiconductor Nanostructures*, edited by D. Bimberg (Springer, Berlin, 2008), p. 123.
- [25] C. Jiang and H. Sakaki, Physica (Amsterdam) **26E**, 180 (2005).